

# Electric Field Induced Permanent Superconductivity in Layered Metal Nitride Chlorides HfNCl and ZrNCl \*

Shuai Zhang(张帅)<sup>1\*\*</sup>, Mo-Ran Gao(高默然)<sup>1,2</sup>, Huan-Yan Fu(傅焕俨)<sup>1,3</sup>, Xin-Min Wang(王欣敏)<sup>1,2</sup>, Zhi-An Ren(任治安)<sup>1,2,4</sup>, Gen-Fu Chen(陈根富)<sup>1,2,4\*\*</sup>

<sup>1</sup>Beijing National Laboratory for Condensed Matter Physics, and Institute of Physics, Chinese Academy of Sciences, Beijing 100190

<sup>2</sup>School of Physical Sciences, University of Chinese Academy of Sciences, Beijing 100049

<sup>3</sup>School of Physics and Electronics, Shandong Normal University, Jinan 250014

<sup>4</sup>Collaborative Innovation Center of Quantum Matter, Beijing 100190

(Received 25 August 2018)

Devices of electric double-layer transistors (EDLTs) with ionic liquid have been employed as an effective way to dope carriers over a wide range. However, the induced electronic states can hardly survive in the materials after releasing the gate voltage  $V_G$  at temperatures higher than the melting point of the selected ionic liquid. Here we show that a permanent superconductivity with transition temperature  $T_c$  of 24 and 15 K is realized in single crystals and polycrystalline samples of HfNCl and ZrNCl upon applying proper  $V_G$ 's at different temperatures. Reversible change between insulating and superconducting states can be obtained by applying positive and negative  $V_G$  at low temperature such as 220 K, whereas  $V_G$ 's applied at 250 K induce the irreversible superconducting transition. The upper critical field  $H_{c2}$  of the superconducting states obtained at different gating temperatures shows similar temperature dependence. We propose a reasonable scenario that partial vacancy of Cl ions could be caused by applying proper  $V_G$ 's at slightly higher processing temperatures, which consequently results in a permanent electron doping in the system. Such a technique shows great potential to systematically tune the bulk electronic state in the similar two-dimensional systems.

PACS: 74.25.-q, 74.62.Bf, 74.25.fc

DOI: 10.1088/0256-307X/35/9/097401

Due to the advantage of easy fabrication process, electric double-layer transistor (EDLT) devices with liquid dielectric have been widely used to tune the carrier density of two-dimensional (2D) materials over a wide doping range. The carrier doped phase always shows dramatic change as compared to parent phase (e.g., metallic state,<sup>[1,2]</sup> magnetic reconstruction<sup>[3,4]</sup> and superconducting (SC) transition<sup>[5–7]</sup>). As one of the most complex physics phenomena, EDLT induced SC transition from insulating parent phase has already become an important topic in condensed matter research. Previous findings in SrTiO<sub>3</sub>,<sup>[5]</sup> ZrNCl<sup>[6,8]</sup> and MoS<sub>2</sub><sup>[7,8]</sup> provide sufficient information and ideas on device design and key parameters such as liquid dielectric and gate voltage  $V_G$ . However, several fundamental requirements must be satisfied to achieve the functional liquid/solid interface.<sup>[9]</sup> First, mechanical micro-cleavage technique is used to prepare ultrathin film with high-quality surface because the carrier depleting and accumulating can occur mainly on surface. Thus, layered crystals with flat surface are more favorable to apply EDLT function.<sup>[6,9,10]</sup> Second, electrodes are patterned on micro-size crystals for electrical transport measurements. Third, as the gate dielectric, proper types of ionic liquids are chosen for applying  $V_G$  without destroying the sensitive crystal surface. Most importantly, the induced SC state remains no longer in the system after releasing the  $V_G$  at

temperatures higher than the melting point of the selected liquid dielectric. All these severe requirements confine the applying of the EDLT method to other systems.

In recent studies, EDLT devices with liquid dielectric have turned into a more powerful technique, which can induce not only the continuous doping of two types of carriers but also the structure transformation. The detailed tuning through the charge density wave (CDW) and superconductivity phase in 1 T-TiSe<sub>2</sub> classified the universality of quantum critical point (QCP).<sup>[11]</sup> A tri-state phase transformation was realized in SrCoO<sub>2.5</sub> by using an electric field to control the insertion and extraction of oxygen and hydrogen ions electrolyzed from H<sub>2</sub>O.<sup>[12]</sup> Upon applying proper  $V_G$ 's, external ions in the dielectric liquid as well as the density of carriers (electrons or holes) in the crystal can be effectively controlled to tune the electronic states. Furthermore, a dual-gate configured device composed of an ionic liquid top gate and a dielectric back gate provides a novel idea on electrostatic control of quantum phases as observed in monolayer WS<sub>2</sub> flakes.<sup>[13]</sup>

As reported in previous studies, upon the intercalation of alkali, alkaline-earth and rare-earth metals, electron doped metal nitride halides MNX ( $M$ : Ti, Zr, Hf;  $X$ : Cl, Br, I) show bulk superconductivity with relatively high  $T_c$  values, 18 K in  $\alpha$ -TiNCl,<sup>[14]</sup> 26 and

\*Supported by the National Natural Science Foundation of China under Grant No 11704403, the National Key Research Program of China under Grant No 2016YFA0401000 and 2016YFA0300604, and the Strategic Priority Research Program (B) of Chinese Academy of Sciences under Grant No XDB07020100.

\*\*Corresponding author. Email: szhang@iphy.ac.cn; gfchen@iphy.ac.cn

© 2018 Chinese Physical Society and IOP Publishing Ltd

15.5 K for  $\beta$ -HfNCl<sup>[15–18]</sup> and ZrNCl,<sup>[19]</sup> respectively. In this study, we carry out detailed experimental studies on layered metal nitride chloride MNCl ( $M$ : Hf and Zr) with applying  $V_G$ 's on submillimeter-scale crystals and polycrystalline samples as shown in Fig. 1. Permanent superconductivity behaviors with  $T_c = 24$  and 15 K are realized on HfNCl and ZrNCl as applying  $V_G$ 's at 250 K, whereas a reversible insulating-SC transition is observed with applying  $V_G$ 's at 220 K. Such unusual behaviors strongly suggest a different mechanism as compared to the normal electrical-double-layer state induced by the gating process. It appears that the electric field induced partial vacancy of Cl could be responsible for the permanent superconductivity observed in the layered metal nitride chlorides.

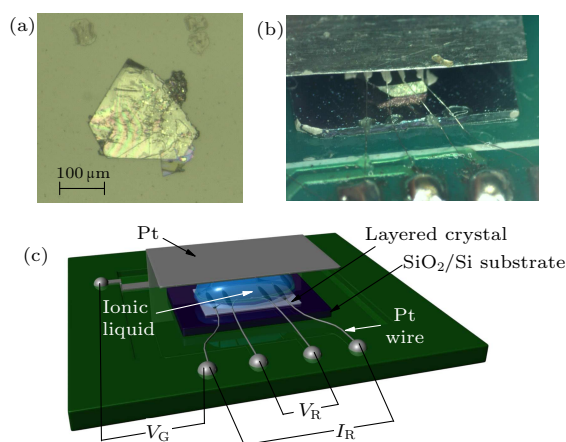


**Fig. 1.** (a) Typical dimensions of the HfNCl single crystals used in this study. (b) A real picture of the self-designed EDLT device with common connecting ports corresponding to standard resistance option on PPMS. (c) Schematic configuration of the EDLT device with ionic liquid filled between submillimeter-scale single crystal and Pt foil. The electrical resistance was measured using the conventional four-probe method with a DC current source in  $I_R$  terminals and voltage sensor between  $V_R$  terminals.

In our experiment, pristine HfNCl and ZrNCl single crystals were grown using the well-established chemical transport method.<sup>[15]</sup> Typical crystal size is  $300 \times 200 \times 10 \mu\text{m}$ . The layered crystals were fixed on a  $\text{SiO}_2$  surface grown on a Si substrate. Normal silver colloid was used to set Pt electrodes for electrical transport measurements as shown in Fig. 1. Lots of tiny single crystals were pressed into pellets with thickness of 0.1–0.2 mm, which were used as the polycrystalline sample. Two typical ionic liquids, i.e., diethylmethyl (2-methoxyethyl) ammonium bis (trifluoromethylsulfonyl) imide (DEME-TFSI) and 1-ethyl-3-methylimidazolium tetrafluoroborate (EMIM- $\text{BF}_4$ ), were chosen as the gate dielectric. The  $V_G$  was applied and kept for 10–30 min at the processing temperature  $T_G = 220$  and 250 K. Compared to conventional field effect transistors, no drain voltage was applied as applying positive/negative  $V_G$ 's between gate (Pt foil, +/–) and source (Pt wire, –/+). The applied  $V_G$  was kept as cooling down the system and was released on the appearance of  $\pm 0.1$  nA of leakage current ( $I_L$ ) near 150 K. The electrical resistance was measured us-

ing the conventional four-probe method with the DC current source as shown in Fig. 1(c), and the temperature dependence of electrical resistance  $R(T)$ 's discussed in the paper were measured in a warming up process.

The temperature dependence of magnetization on the same single crystals was measured after completing the electrical transport measurements. After reapplying proper  $V_G$ 's at the corresponding temperatures (5.5 V at 220 K and 3.5 V at 250 K), the system was warmed up to room temperature, and the same single crystals were cleaned and transferred to magnetization measuring system using an SQUID magnetometer (Quantum Design SQUID VSM). Because of the unmeasurable mass of single crystals ( $\leq 0.1$  mg), the slight error was unavoidable due to the weak magnetization signal, which is close to the measurement accuracy. However, the SC transitions can still be clearly determined.

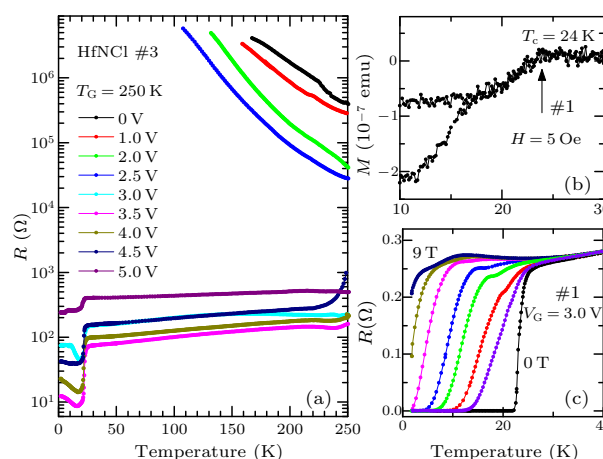


**Fig. 2.** Electric field induced permanent superconductivity with  $T_c = 24$  K in the layered HfNCl single crystals. The  $V_G$ 's were applied at 250 K. (a) Temperature dependence of resistance  $R(T)$  at  $V_G$ 's from 0 to 5 V. (b) Temperature dependence of magnetization  $M(T)$  of the same single crystal (#1) after completing the  $R(T)$  measurements. (c) Temperature dependence of  $R(T)$  under different magnetic fields ( $\mu_0 H = 0, 0.5, 1, 2, 3, 5, 7, 9$  T) with  $V_G = 3.0$  V.

Figure 2(a) shows a series of temperature dependence of resistance  $R(T)$ 's measured after applying different  $V_G$ 's at processing temperature  $T_G = 250$  K. The  $R(T)$  curves line up in two groups: typical insulating  $R(T)$  for  $V_G \leq 2.5$  V and metallic  $R(T)$  for  $V_G \geq 3$  V. For the insulating  $R(T)$  groups, the absolute value of resistance decreases monotonically with increasing  $V_G$ , implying the increase of carrier density in the system. An apparent insulator-metal transition with the decrease of resistance in four orders of magnitude occurs between  $V_G = 2.5$  and 3 V. The steep drop around 25 K observed in  $R(T)$  with  $V_G \geq 3$  V corresponds to the SC transition, which is also confirmed in the temperature dependence of magnetization  $M(T)$  (Fig. 2(b)) and  $R(T)$  under magnetic fields (Fig. 2(c)). The transition temperature  $T_c$  is determined to be 24 K using the conventional extrapolation method, and the zero resistance at 22.2 K is higher

than all the reported values for intercalated superconductors  $A_x\text{HfNCI}$  with/without cointercalation of molecules.<sup>[15,17,19]</sup> The confirmation of  $T_c$  in  $M(T)$  proves directly the permanent characteristic of the SC

state after releasing the  $V_G$ , which is strongly contrast to the general EDLT function induced superconductivity.

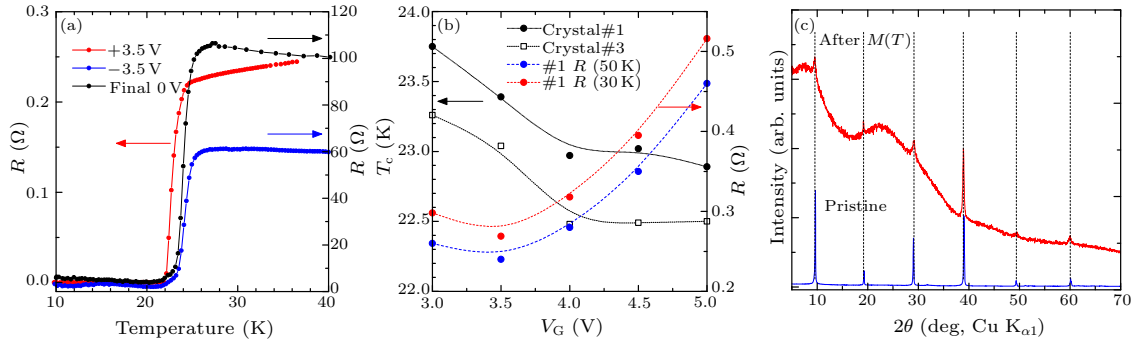


**Fig. 3.** (a) Temperature dependence of electrical resistance  $R(T)$  of HfNCI after applying positive, negative and zero  $V_G$  at processing temperature  $T_G = 250$  K. (b) Gate voltage  $V_G$  dependence of the induced  $T_c$  (left scale) and absolute resistance  $R(30\text{K})$  and  $R(50\text{K})$  (right scale). (c) The XRD pattern of the same layered HfNCI crystal before and after all  $R(T)$  and  $M(T)$  measurements.

To dynamically probe the electric field induced permanent SC state,  $V_G$  of  $-3.5$  and  $0$  V was applied after completing the  $R(T)$  measurements with  $V_G = 5$  V. As compared to the  $R_{V_G=3.5\text{V}}(T)$  in Fig. 3(a), the onset of  $T_c$  increases slightly, and the absolute resistance is increased by two orders of magnitude. The applying of negative  $V_G$  and/or long-time relaxation without  $V_G$  at the same temperatures (250 K) can hardly destroy the induced SC state. Note that the SC transition is reconfirmed in  $M(T)$  after several-week relaxation in the Ar gas filled glove box, suggesting again that the induced SC states remain permanently in the material. Figure 3(b) shows the  $V_G$  dependence of  $T_c$  observed on single crystals #1 and #3. With increasing  $V_G$  from 3 to 5 V, near 1 K weakening of  $T_c$  is confirmed on all selected crystals with good reproducibility. The  $V_G$  dependence of  $T_c$  is consistent with the  $T_c$  depending on doping level observed on bulk intercalated superconductors such as  $\text{Li}_x\text{M}_y\text{HfNCI}$ <sup>[19]</sup> and  $\text{AE}_x\text{M}_y\text{HfNCI}$ .<sup>[17]</sup> Meanwhile, the resistances  $R(30\text{K})$  and  $R(50\text{K})$  start to increase with increasing  $V_G$  above 3.5 V, which suggests that optimal  $V_G$  for the sheet conductivity occurs around this area. With increasing  $V_G$ ,  $T_c$  decreases monotonically, which suggests a monotonic increase of the doped carrier density. Both the increase of  $R$  and the decrease of  $T_c$  at high  $V_G$  region imply a developed scattering at a high doping level.

One of the typical characteristics of the layered  $\text{MNCl}$  system is the large interlayer distance, which allows the intercalation of various metals with/without molecules.<sup>[15–18]</sup> The XRD pattern of the single crystals was measured before and after all the  $R(T)$  and  $M(T)$  measurements. As shown in Fig. 3(c), the  $[001]$  reflection peaks in the XRD pattern show no apparent shift compared to the pristine single crystal, which could exclude the possibility of intercalation of large-size ions from liquid dielectric. Because the crystal surfaces were cleaned after the

electrical transport measurements, the poor intensity of the reflection peaks could imply that some changes on crystal surfaces were caused in the gating process.

To clarify the difference between the intrinsic mechanisms of the present findings on bulk single crystals and the previous studies on atomically flat films of  $\text{ZrNCI}$ ,<sup>[6,8]</sup> we verify the EDLT function on  $\text{ZrNCI}$  with applying  $V_G$  at  $T_G = 220$  K (LT) and 250 K (HT). Figures 4(a) and 4(b) show the systematic  $R_{\text{HT}}(T)$  and  $R_{\text{LT}}(T)$  behaviors at different  $V_G$ 's. At 220 K, the EDLT induced insulating-SC transition around 15 K is in great agreement with the previous results observed on atomically flat films; the absolute resistance decreases monotonically with increasing  $V_G$ . As discussed in the following, the applying of negative  $V_G$  and/or long-time relaxation without  $V_G$  at 220 K recovers the system from SC to the insulating-like state. On the other hand, for  $T_G = 250$  K,  $R_{\text{HT}}(T)$  at  $V_G = -2$  and  $-4$  V shows no change compared to  $V_G = 0$  V. With increasing positive  $V_G$ , absolute resistance decreases monotonically between 0 and 3.5 V, and increases again from 3.5 to 5.5 V. The overall tendency of  $R_{\text{HT}}(T)$  reproduces fully the observations on HfNCI discussed previously (Fig. 3(b)), strongly implying that the processing temperature at which  $V_G$ 's were applied plays a dominant role in the electric field induced superconductivity. Note that  $R(T)$ 's with the same  $V_G$  applied at 220 and 250 K show intrinsic difference in both low- and high- $V_G$  regions.

The transition temperature  $T_c$  is clearly determined in low-temperature  $R(T)$  as shown in Fig. 4(c). At  $V_G = 2.5$  V, two clear transitions were confirmed at  $T_{c1}$  and  $T_{c2}$ , which are similar to the previous observations on  $\text{ZrNCI}$ .<sup>[6]</sup> We consider that such a two-step transition could be caused by the nonhomogeneity of the transport channel. The  $T_{c1}$  and  $T_{c2}$  values determined in  $R(T)$  with applying  $V_G$  at both 220 and 250 K are summarized in Fig. 4(d). All the values of  $T_c$  display a rather weak  $V_G$  dependence.  $T_c$  de-

increases monotonically with increasing  $V_G$ , showing an agreement with the carrier doping level dependence of  $T_c$  observed on bulk intercalated superconductors,<sup>[20]</sup> whereas the previous gating experiments on atomically flat films of ZrNCl show a different  $V_G$  dependence of  $T_c$ .<sup>[6]</sup>

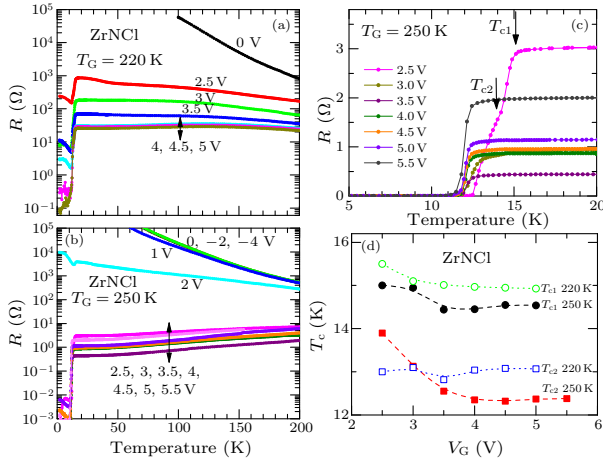


**Fig. 4.** Intrinsic difference of the superconductivity induced by applying  $V_G$  at different processing temperatures. Systematic temperature dependence of resistance  $R(T)$  with applying  $V_G$  at 220 K (a) and 250 K (b). (c) The  $T_c$  is clearly identified in low-temperature  $R(T)$ . (d) The  $V_G$  dependence of induced  $T_{c1}$  and  $T_{c2}$  observed in  $R(T)$  with applying  $V_G$  at 220 and 250 K.

Negative voltages were applied to probe the difference between applied  $V_G$ 's at 220 and 250 K as shown in Fig. 5(a) and 5(b), respectively. Upon applying  $V_G = -5$  V at 220 K for several hours after measurements at  $V_G = +5.5$  V,  $R_{LT}(T)$  could be restored to thousands of ohm at low temperatures. Several-day relaxation without applying  $V_G$  at room temperature could restore  $R(T)$  to the insulating state. Although the continuous recovery from SC to insulating state is quite time-consuming, the induced electronic state disappears as releasing the  $V_G$  at temperatures higher than the melting point of the selected liquid dielectric, which is similar to the general EDLT induced behavior. In contrast, the  $T_c$  induced by applying  $V_G$  at 250 K increases up to  $\sim 15.3$  K with applying  $-5$  V and/or long-time relaxation without  $V_G$  at the same temperature (250 K). Meanwhile, the absolute value of  $R_{HT}(T)$  shows an increase of more than ten times as well as the disappearance of the two-step transition. We conclude that the applying of negative  $V_G$  contributes to the relaxation of electronic state induced as applying  $V_G$  at 250 K. The similar behavior was also observed on HfNCl as shown in Fig. 3(a).

As a double check, temperature dependence of magnetization  $M(T)$  was measured on the same single crystals of ZrNCl (see the above experimental details). The single crystals with applying  $V_G$  at  $T_G = 250$  and 220 K are named the HT and LT crystals, respectively. As shown in Fig. 5(c),  $M(T)$  of the HT crystal shows a clear SC transition around 15 K, whereas no transition is confirmed down to 1.8 K for the LT crystal, implying the permanent superconductivity in

the former case. Such experimental facts are in great agreement with the observations in HfNCl discussed previously. Furthermore, taking the advantage of the layered characteristic in the present system, we have successfully extended the gating function to the polycrystalline samples using different types of ionic liquids (DEME-TFSI and EMIM-BF<sub>4</sub>). The same gating processing was applied at 250 K on the polycrystalline samples. As shown in Fig. 5(d),  $M(T)$  shows clear SC transitions with  $T_c = 15.3$  K, and the induced SC transitions are consistent with the bulk superconductivity observed on intercalated superconductors.

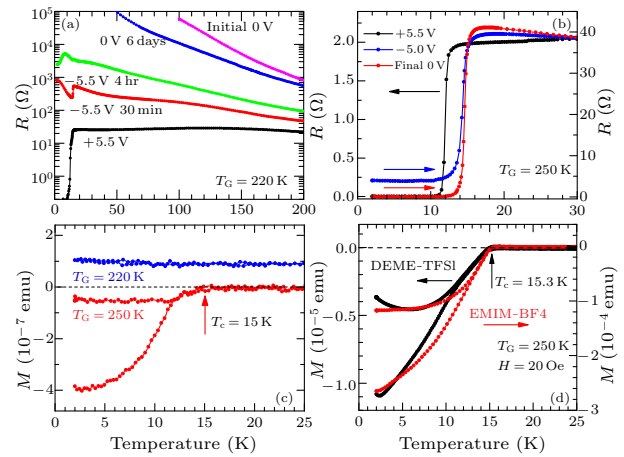


**Fig. 5.** Reversible and irreversible  $R(T)$  with applying  $V_G$  at different temperatures. At  $T_G = 220$  and 250 K (b), temperature resistance dependence of resistance  $R(T)$  shows reversible and irreversible insulating-SC transition as applying negative  $V_G$ 's. (c) Temperature dependence of magnetization  $M(T)$  of the same single crystal used in  $R(T)$  measurements. (d) The EDLT function has been successfully extended to millimeter-scale polycrystalline samples using different ionic liquid (DEME-TFSI and EMIM-BF<sub>4</sub>). The induced SC transition is confirmed around 15 K in the temperature dependence of magnetization  $M(T)$ .

To discuss the difference of superconductivity induced by applying  $V_G$  at 220 and 250 K, we show the systematic results of  $R(T)$  (Fig. 6(a) and 6(b)),  $R(H)$  (Fig. 6(c)) and a summarized  $H$ - $T$  phase diagram (Fig. 6(d)).  $R(T)$  was measured in the configuration of  $H \perp I \parallel ab$ . The metallic feature was observed by applying  $V_G$  of 5 V at 220 K and 2.5 V at 250 K, which show the similar  $T_c$  value of 15 K. Thus, the response to magnetic fields was studied on these two similar SC states. With applying magnetic fields up to 3 T, the SC transition temperature  $T_c$  decreases monotonically. A higher magnetic field ( $> 3$  T) leads to a constant resistance without apparent dependence on temperature or magnetic field. Meanwhile, as shown in Fig. 6(c), the isothermal field dependence  $R(H)$  at 2 K shows that zero resistance remains in fields less than 0.7 T, which is followed by a wide up-turn between 0.7 and 3 T and a flat resistance above 3 T. Except for the difference on the absolute value of resistance, the overall tendencies of  $R(T)$  and  $R(H)$  show no obvious difference between the two SC states induced at  $T_G = 220$  and 250 K. The upper critical field  $H_{c2}$  was estimated using the  $R(T)$  in different

magnetic fields. The determined  $H_{c2}$  values are summarized in Fig. 6(d), in which the  $H_{c2}$  values reported in the previous studies are plotted together.<sup>[6,20]</sup> Obviously, the  $H_{c2}$  estimated in the present study shows no difference in SC states induced by applying  $V_G$  at 220 and 250 K, which are in great agreement with the previous finding observed on atomically flat films of ZrNCl.<sup>[6]</sup>

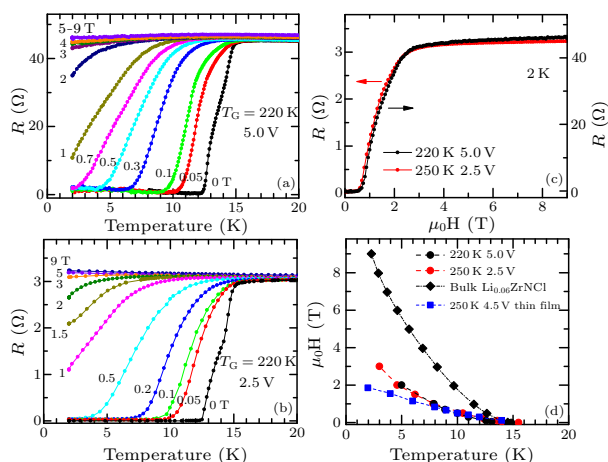


**Fig. 6.** Temperature dependence of resistance  $R(T)$  of ZrNCl under magnetic fields as applying  $V_G = 5$  V at  $T_G = 220$  (a) and  $V_G = 2.5$  V at 250 K (b), respectively. (c) Isothermal field dependence of resistance  $R(H)$  at 2 K. (d)  $H_{c2}(T)$  with  $H \perp I \parallel ab$  estimated from  $R(T)$  under magnetic fields, which are compared to the previous findings on ZrNCl.<sup>[20,6]</sup>

Here we attempt to discuss the mechanism of the

electric field induced permanent superconductivity on layered  $MNCl$  ( $M$ : Hf and Zr). The electrochemical window (EW) is a key parameter depending on temperature. Based on the previous studies using DEME-TFSI,<sup>[1,6,21]</sup>  $\pm 5$  V is allowed at 220 K. With increasing temperature up to 250 K, the EW decreases and the ionic liquid could be destroyed by the  $V_G$  as high as 5 V. The decomposition of the ionic liquid leads to some kind of ions/atoms with small ionic/atomic sizes, which could be intercalated in the layered crystals, consequently a permanent SC state forms from the intercalation effect on bulk crystals. However, this possible process is contradictory with the experimental fact such as the irreversible insulating-SC transition with applying negative  $V_G$ . In general, electric field induced intercalation could be recovered upon applying reverse  $V_G$  as observed in recent studies on field-driven proton injection.<sup>[12,22]</sup> On the other hand, no apparent anomaly was found in the  $I_L-t$  curve as applying  $V_G$  of 5 V at 250 K. Furthermore, lots of studies have reported that the EW of DEME-TFSI at room temperature is between +3 and -3.<sup>[1,23]</sup> The EW increases with decreasing temperature so that the EW of DEME-TFSI at 250 K should be between 3 and 5 V. Note that  $R(T)$  with  $V_G$  as small as 2.5 V applied at 220 and 250 K shows semiconductor-like (Fig. 4(a)) and metallic (Fig. 4(b)) temperature dependences with difference of nearly two orders of magnitude in absolute resistance. Such results have high reproducibility and can hardly be considered as sample dependence.

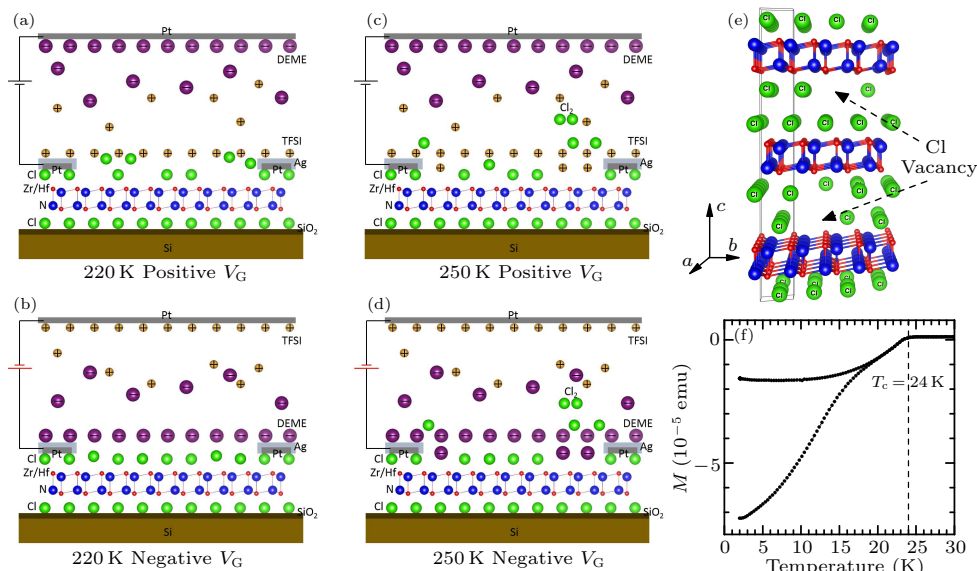


**Fig. 7.** Concept of electric field induced phase transformation. Reversible phase transformation obtained by applying positive (a) and negative  $V_G$  (b) at 220 K. Irreversible phase transformation occurs as applying positive (c) and negative  $V_G$  (d) at higher temperatures such as 250 K. (e) The structure model with electric field induced Cl vacancies. (f) The diamagnetism corresponding to SC transition observed in  $M(T)$  of a polycrystalline sample.

Based on all experimental facts obtained in the present study, we propose a reasonable scenario interpreting the difference between applying  $V_G$  at 220 and

250 K. Upon applying  $V_G$  at 220 K (Fig. 7(a)), short-range movement of partial  $Cl^{1-}$  ions could be induced by the positive  $V_G$ , leading to a local electron doping

in the system. The applying of reverse  $V_G$  and/or prolonged relaxation can almost push back the Cl ions to the initial positions (Fig. 7(b)). This is consistent to the electric field induced SC transition and restored insulating state (Fig. 5(a)). The conventional EDLT effect can also explain the reversible insulating-SC transition observed at 220 K. On the other hand, for applying  $V_G$  at 250 K, partial  $\text{Cl}^{1-}$  ions could get enough energy to escape from the crystal surface (Fig. 7(c)). The boiling temperature of  $\text{Cl}_2$  is near 240 K. The possible formation of  $\text{Cl}_2$  can provide extra electrons, which results in a permanent electron doping to the system. The silver particles around the electrodes may assist this chemical process. Correspondingly, the reverse  $V_G$  contributes to the improvement of the homogeneity more than pushing back the Cl ions to the system (Fig. 7(d)). Thus, the permanent superconductivity observed in the present study could be caused by the partial vacancy of Cl as observed in the deintercalation experiments on bulk  $\text{MnCl}$  crystals.<sup>[24]</sup> The gating process with high  $V_G$  near the EW limit at 250 K could be responsible for the irreversible chemical reaction such as the vacancy formation of Cl. The similar process was previously observed on  $\text{VO}_2$  films. A considerable suppression of metal-insulator transition was caused by electric field-induced oxygen vacancy formation.<sup>[25]</sup> Furthermore, it was reported that the  $\text{VO}_2$  films were seriously damaged by applying the low  $V_G$  (2 V) at room temperature for several hours.<sup>[26]</sup>

As discussed above, for both  $\text{HfNCl}$  and  $\text{ZrNCl}$ , reverse  $V_G$  results in the increase of  $T_c$  and absolute resistance  $R(T)$  (Figs. 3(a) and 5(b)), which can also be interpreted by the proposed model. The poor homogeneity of the transport channel is caused by the random deintercalation of Cl. Upon applying negative  $V_G$ 's and/or long-time relaxation at high temperature without  $V_G$ , the local high density of Cl vacancies may turn into relatively uniform low density of vacancies, which is equal to the change from local high doping level to uniform low carrier density. Correspondingly, the  $T_c$  increases with the decreasing carrier density, which is consistent with the observations on bulk superconductors.<sup>[19]</sup> In the meantime, the local strong scattering turns into a relatively uniform weak scattering, which is responsible for the increase of absolute  $R(T)$ . We consider that such a process is a dynamic relaxation especially under negative  $V_G$ 's.

Upon optimization of all variable parameters in the gating process, we have obtained a clear and permanent SC states in  $\text{HfNCl}$  as shown in Fig. 7(f). As already mentioned before, the EDLT induced SC state occurs mainly on crystal surface, and has poor homogeneity. Thus, partial deintercalation of Cl occurs randomly on the crystal surfaces, which is also evidenced by the absent color change of the crystals after processing EDLT function. The vacancy with a relative uniform distribution could result in a primary phase of  $\text{HfNCl}_{1-x}$  (Fig. 7(e)). As shown in Fig. 7(f), SC transition at 24 K is confirmed in  $M(T)$ , which is consistent with the results on single crystals (Fig. 2(b))

and bulk deintercalated samples.<sup>[24]</sup> The strong magnetization signal obtained on a thick polycrystalline sample of  $\text{HfNCl}$  strongly supports that the electric-field-driven deintercalation is not limited by the requirements for EDLT devices.

In summary, we unfold a connection between traditional solid-state synthesis and electric field induced chemical reaction on layered  $\text{MNCl}$  ( $M$ : Hf and Zr) crystals. Compared to the strongly bonded honeycomb-like double  $[\text{MN}]$  layers, the interaction between chlorine and  $[\text{MN}]$  layers is relatively weak. Upon applying positive and negative  $V_G$  at low temperature such as 220 K, system shows a reversible change between insulating and SC states, whereas the EDLT function applied at 250 K results in the irreversible SC transition with  $T_c = 24$  and 15 K on  $\text{HfNCl}$  and  $\text{ZrNCl}$ , respectively. Such findings imply that the electric field induced partial vacancy of Cl ions could be responsible for the permanent superconductivity. The discovery of such an electrochemical mechanism of permanent superconductivity will shed light on tuning bulk electronic states in similar 2D systems using EDLT devices.

## References

- [1] Yuan H T, Shimotani H, Tsukazaki A, Ohtomo A, Kawasaki M and Iwasa Y 2009 *Adv. Funct. Mater.* **19** 1046
- [2] Leng X, Pereiro J, Strle J, Dubuis G, Bollinger A T, Gozar A, Wu J, Litombe N, Panagopoulos C, Pavuna D and Božović I 2017 *npj Quantum Mater.* **2** 35
- [3] Yuan H T, Bahramy M S, Morimoto K, Wu S F, Nomura K, Yang B J, Shimotani H, Suzuki R, Toh M, Kloc C, Xu X, Arita R, Nagaosa N and Iwasa Y 2013 *Nat. Phys.* **9** 563
- [4] Zhang Z C, Feng X, Guo M H, Li K, Zhang J S, Ou Y B, Feng Y, Wang L L, Chen X, He K, Ma X C, Xue Q and Wang Y Y 2014 *Nat. Commun.* **5** 4915
- [5] Ueno K, Nakamura S, Shimotani H, Ohtomo A, Kimura N, Nojima T, Aoki H, Iwasa Y and Kawasaki M 2008 *Nat. Mater.* **7** 855
- [6] Ye J T, Inoue S, Kobayashi K, Kasahara Y, Yuan H T, Shimotani H and Iwasa Y 2010 *Nat. Mater.* **9** 125
- [7] Ye J T, Zhang Y J, Akashi R, Bahramy M S, Arita R and Iwasa Y 2012 *Science* **338** 1193
- [8] Saito Y, Nojima T and Iwasa Y 2018 *Nat. Commun.* **9** 778
- [9] Ueno K, Shimotani H, Yuan H, Ye J, Kawasaki M and Iwasa Y 2014 *J. Phys. Soc. Jpn.* **83** 032001
- [10] Lei B, Cui J H, Xiang Z J, Shang C, Wang N Z, Ye G J, Luo X G, Wu T, Sun Z and Chen X H 2016 *Phys. Rev. Lett.* **116** 077002
- [11] Li L J, O'Farrell E C T, Loh K P, Eda G, Ozyilmaz B and Castro Neto A H 2016 *Nature* **529** 185
- [12] Lu N P, Zhang P F, Zhang Q H, Qiao R M, He Q, Li H B, Wang Y J, Guo J W, Zhang D, Duan Z, Li Z L, Wang M, Yang S Z, Yan M Z, Arenholz E, Zhou S Y, Yang W L, Gu L, Nan C W, Wu J, Tokura Y and Yu P 2017 *Nature* **546** 124
- [13] Lu J M, Zheliuk O, Chen Q H, Leermakers I, Hussey N E, Zeitler U and Ye J T 2018 *Proc. Natl. Acad. Sci. USA* **115** 3551
- [14] Zhang S, Tanaka M and Yamanaka S 2012 *Phys. Rev. B* **86** 024516
- [15] Yamanaka S, Hotehama K and Kawaji H 1998 *Nature* **392** 580
- [16] Ye G J, Ying J J, Yan Y J, Luo X G, Cheng P, Xiang Z J, Wang A F and Chen X H 2012 *Phys. Rev. B* **86** 134501
- [17] Zhang S, Tanaka M, Zhu H and Yamanaka S 2013 *Supercond. Sci. Technol.* **26** 085015

- [18] Zhang S, Tanaka M, Onimaru T, Takabatake T, Isikawa Y and Yamanaka S 2013 *Supercond. Sci. Technol.* **26** 045017
- [19] Takano T, Kishiume T, Taguchi Y and Iwasa Y 2008 *Phys. Rev. Lett.* **100** 247005
- [20] Taguchi Y, Kitora A and Iwasa Y 2006 *Phys. Rev. Lett.* **97** 107001
- [21] Yuan H T, Liu H W, Shimotani H, Guo H, Chen M W, Xue Q K and Iwasa Y 2011 *Nano Lett.* **11** 2601
- [22] Cui Y, Zhang G H, Li H B, Lin H, Zhu X Y, Wen H H, Wang G G, Sun J Z, Ma M W, Li Y, Gong D L, Xie T, Gu Y H, Li S L, Luo H Q, Yu P and Yu W Q 2018 *Sci. Bull.* **63** 11
- [23] Sato T, Masuda G and Takagi K 2004 *Electrochim. Acta* **49** 3603
- [24] Zhu L and Yamanaka S 2003 *Chem. Mater.* **15** 1897
- [25] Jeong J, Aetukuri N, Graf T, Schladt T D, Samant M G and Parkin S S P 2013 *Science* **339** 1402
- [26] Zhou Y and Ramanathan S 2012 *J. Appl. Phys.* **111** 084508